

EVOLUTION OF MASSIVE STARS INTO LUMINOUS BLUE VARIABLES AND
WOLF-RAYET STARS FOR A RANGE OF METALLICITIES:
THEORY VERSUS OBSERVATION

RICHARD B. STOTHERS AND CHAO-WEN CHIN

Institute for Space Studies, NASA/Goddard Space Flight Center, 2880 Broadway, New York, NY 10025

Received 1996 January 2; accepted 1996 March 21

ABSTRACT

Evolutionary tracks for 30–90 M_{\odot} stars, computed along the lines described in our recent series of papers, suggest that luminous blue variables (LBVs) are the blue remnants of a prior phase of heavy mass loss. They are now intermittently experiencing ionization-induced dynamical instability within their hydrogen-poor envelopes, while their massive helium cores are in an advanced stage of central helium burning. In the H-R diagram, our new evolutionary models successfully explain the high- and low-temperature limits, the low-luminosity limit, and the relative luminosity function of the observed LBVs at quiescence which have $\log(L/L_{\odot}) < 6.3$. Metal-poor LBVs are predicted (correctly, in the only case known) to be significantly cooler than LBVs with normal metallicities. In the (mass, luminosity) plane, the models and observed stars agree closely, and show no discernible metals dependence. Predicted values of the surface hydrogen abundance and of the expelled mass during the LBV phase match reasonably well the available observational data, which, however, are still very crude. The observed cycles of mass loss are predicted correctly. Pre-LBV and post-LBV stars can be identified with the hydrogen-poor and hydrogen-free WN stars, respectively. Post-red-supergiant lifetimes, derived from published star counts and kinematical ages of nebulae around the WN stars and LBVs, are used to infer an approximate mean value of the rate of stellar wind mass loss from luminous red supergiants. This parameter is crucial for understanding stellar evolution at $\log(L/L_{\odot}) < 5.8$. Stars more luminous may never become red, and may spend all, or nearly all, of their post-main-sequence lives as blue supergiants. Our theory of LBVs makes a number of other predictions that have not yet been tested. A critical comparison with the very different theory of Langer et al. is presented.

Subject headings: stars: evolution — stars: oscillations —

stars: variables: other (luminous blue variables) — stars: Wolf-Rayet — supergiants

1. INTRODUCTION

Stars now designated as “luminous blue variables” (LBVs) occupy the hot, bright portion of the Hertzsprung-Russell (H-R) diagram and exhibit conspicuous light and color variations that arise from their expelled circumstellar shells (Conti 1984). The distribution of LBVs on the H-R diagram during states of quiescence is reasonably well delineated for objects with an approximately solar metals abundance (Humphreys & Davidson 1994). How this distribution changes with metallicity, however, is a question that is just beginning to be answered. Before the recent recognition of R40 in the Small Magellanic Cloud (SMC) as an LBV (Szeifert et al. 1993), no member of this class had been identified in a metal-poor galactic environment. It had been supposed either that the smallness of the stellar population in the searched metal-poor galaxies was responsible for an apparent lack of LBVs (Humphreys 1989) or that a low metallicity somehow prevented a massive star from evolving into a LBV (Wolf 1991). Although R40 now changes the situation, a new question arises.

The physical mechanism that we recently proposed to explain those LBVs that have approximately solar metallicities does not, at first sight, work for stars with much lower metallicities (Stothers & Chin 1993, hereafter SC93). Our mechanism consists of a classical, ionization-induced dynamical instability that occurs in the outer layers of the star where the ionization zones of hydrogen and helium are located. A necessary auxiliary condition is that an extremely high radiation pressure exist just below these zones. In stars of high mass this condition is brought about by a large

opacity due mostly to multiple iron lines (Iglesias, Rogers, & Wilson 1992) formed at temperatures around 2×10^5 K. If the initial metals abundance is low, the iron opacity “bump” is small, and radiation pressure accordingly decreases in importance.

A very high radiation pressure, however, depends also on having a large luminosity-to-mass ratio in the outer envelope. This ratio is increased by mass loss from the stellar surface. With enough mass loss, the disadvantage created by a low initial metals abundance might be overcome.

One purpose of the present paper is to determine precisely under what physical conditions our proposed mechanism for LBVs with normal metallicities can work for metal-poor LBVs. To achieve a better model comparison, we have also broadened our investigation of LBVs with normal metallicities. With all these theoretical data in hand, a detailed confrontation of the stellar models can be made with observations of the quiescent states of LBVs.

The present study is the fourth in a series that includes the original presentation of our new physical mechanism (SC93), our report on a second phase of dynamical instability that applies to essentially all of the known LBVs (Stothers & Chin 1994, hereafter SC94), and our detailed investigation of the conspicuous, slow cycles shown by these variables (Stothers & Chin 1995, hereafter SC95). The number and variety of the many points of quantitative agreement between our models and the observations, employing a definite mechanism for the eruptive mass loss, have not been duplicated by any other theoretical explanations of the LBVs. Advantages and disadvantages of our

proposed theory with respect to the very different scenarios proposed by other authors are discussed at the end of the paper.

2. PHYSICAL ASSUMPTIONS

Physical input parameters are the same as those adopted in our original study (SC93), except that we have now increased the range of assigned metallicities. Initial (hydrogen, metals) abundances by mass are taken here to be $(X, Z) = (0.700, 0.03), (0.756, 0.004),$ and $(0.758, 0.002)$.

For all stars except the coolest, the stellar wind mass-loss rates are assumed to be either the formula-fitted observational rates of Nieuwenhuijzen & de Jager (1990) or, as in our earlier study, those rates multiplied by $(Z/0.03)^{0.8}$, which incorporates the theoretically calculated dependence of the rates on metallicity (Leitherer, Robert, & Drissen 1992). Since the rates of stellar wind mass loss are in any case uncertain by a substantial factor for extremely massive hot stars (Lamers & Leitherer 1993), we are probably justified in employing the unmodified Nieuwenhuijzen & de Jager rates as an *upper limit* for metal-poor stars. The uncertainty in these rates has importance only when the initial mass exceeds $\sim 60 M_{\odot}$.

On the red side of the H-R diagram, the Nieuwenhuijzen & de Jager rates are uncertain by a factor of about 10 either way (Dupree 1986, Fig. 13; Jura & Kleinman 1990). To evolve a star of initially $30 M_{\odot}$ out of this region, as observations require, necessitates somewhat higher than standard rates. We have arbitrarily adopted a multiplicative factor of 5, although a factor of ~ 2 would do, and would in fact have been preferable (§ 7). For consistency, we have adopted the same multiplicative factor of 5 at all masses. With or without such an enhancement factor, few (if any) red supergiants would be theoretically expected to exist at luminosities greater than $\log(L/L_{\odot}) = 5.8$, which represents the brightest red supergiants known (Humphreys & Davidson 1994).

Dynamical instability in the outer envelope undoubtedly induces much heavier mass loss, but an accurate rate has not yet been determined either from observations or from nonlinear hydrodynamical calculations (SC93). When the star is red, any assigned large rate (up to as much as $10^{-1} M_{\odot} \text{ yr}^{-1}$) yields very nearly the same final model. When the star becomes blue later, the prevailing rate can be inferred from the theoretical requirement that rapid cycling between dynamically stable and unstable states should occur in order to reproduce the observed LBV cycles (SC95). If the assigned rate is too large, the star stays blue and does not evolve redward to the threshold of dynamical instability; if the rate is too small, the star continues evolving redward and fails to return promptly to a blue, dynamically stable state. The range of acceptable rates turns out to be quite limited and in agreement with the rough observed values. During the quiescent phase of a cycle, the exact size of the stellar wind mass loss rate is unimportant for determining the properties of the cycle, and can be assigned a value as small as zero or as large as a quarter of the eruptive mass-loss rate without sensibly altering the results. This is wholly consistent with the otherwise puzzling observation that LBV eruptions sometimes occur even when the eruptive mass-loss rate is only slightly larger than the quiescent rate (Lamers 1989).

The criterion for dynamical instability which is applied to our models is that $\langle \Gamma_1 \rangle$, the pressure-weighted volumetric

average of the first generalized adiabatic exponent in the outer envelope, must be less than $4/3$. Strictly speaking, this simple criterion, which is easy to compute from a quasi-hydrostatic stellar model, applies only when the radius displacements are homologous (Ledoux 1958). However, the exact eigenfunctions that we have computed by solving the linear adiabatic radial wave equation governing dynamical instability show that this approximation is reasonably good and that the approximate and exact solutions yield very nearly the same point of onset of dynamical instability along an evolutionary track. Since a large ratio of radiation pressure to gas pressure lowers Γ_1 close to $4/3$ and the partial ionization of hydrogen and helium reduces Γ_1 below $4/3$, these two factors together are responsible for bringing the *average* value of Γ_1 in the outer envelope below $4/3$. A high radiation pressure occurring just below the hydrogen and helium ionization zones also serves to isolate the outer envelope layers structurally from the rest of the star. All of these conditions are necessary to trigger an actual outbreak of dynamical instability (SC93).

3. EVOLUTION OF MASSIVE STARS WITH NORMAL METALLICITIES

We begin by recapitulating the results that we have already obtained for the evolution of massive stars with normal metallicities. If the star's initial mass is greater than $\sim 60 M_{\odot}$, dynamical instability develops shortly after the main-sequence phase while the star is rapidly crossing the yellow portion of the H-R diagram. Nearly all of the hydrogen envelope is quickly stripped off. The remnant then settles down into the slow phase of central helium burning on the blue side of the H-R diagram. Eventually, there is a move toward the red region again, but the star runs into dynamical instability at about the same position where it terminated dynamical instability the first time around. Repeated shell ejections occur until the stellar envelope becomes so reduced in mass that either the star can no longer expand redward or its remaining hydrogen content is too small to maintain the requisite high radiation pressure for dynamical instability to occur (§ 4).

In the case of initial stellar masses between $\sim 30 M_{\odot}$ and $\sim 60 M_{\odot}$, the pattern of evolution is somewhat similar, but the star remains dynamically stable until long after leaving the main sequence. The star thus immediately acquires a stable red supergiant configuration and begins to deplete core helium. If the rate of stellar wind mass loss is sufficiently high, the star eventually loses most of its hydrogen envelope and then moves quickly into a blue configuration. The final stages of mass loss in the red region *may* be accompanied by dynamical instability, although the smallest initial mass for this to happen depends on the prior rate of stellar wind mass loss; for our present models the critical initial mass is $\sim 35 M_{\odot}$. When dynamical instability occurs, a very rapid transition, much like that for a low-mass star during the formation of a planetary nebula, takes place.

Figure 1 illustrates the three basic types of evolution on the H-R diagram, for initial stellar masses of 30, 45, and $90 M_{\odot}$. We caution that the computed lengths and durations of the post-red-supergiant blue loops in the present tracks are unreliable for making detailed quantitative comparisons with observations. These two properties of the blue loops depend very strongly on the uncertain rates of stellar wind mass loss during the star's previous red supergiant history.

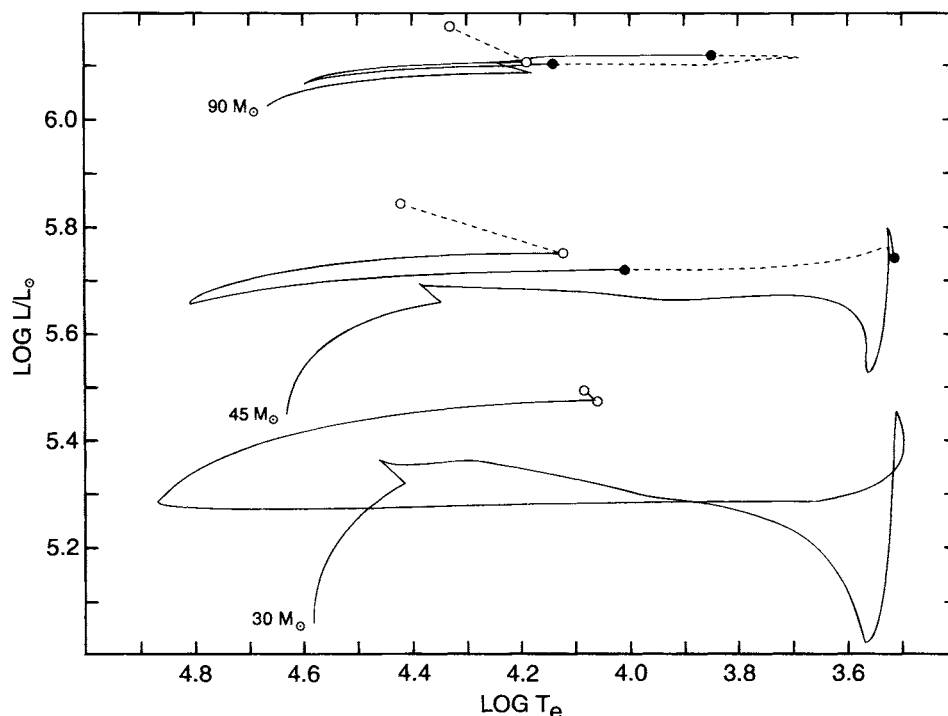


FIG. 1.—Theoretical H-R diagram showing evolutionary tracks for $Z = 0.03$, running from the zero-age main sequence (initial stellar mass indicated) to the end of the second (blue) phase of dynamical instability. Dashed portions of the evolutionary track connect the starting and terminating points of the first (yellow or red) phase of dynamical instability (filled circles) and of the second (blue) phase (open circles). Individual cycles occurring both during the blue phase and near the end of the yellow phase usually show very small amplitudes and so are not displayed. Maximum effective temperatures achieved along the post-red-supergiant evolutionary blue loops have a large uncertainty.

This drawback is discussed in more detail in § 7, where we show that a plausible way exists to get round the problem.

Nonetheless, the computed H-R diagram location of the *start* of the blue phase of dynamical instability is relatively well-determined. The reason is that, in order to have dynamical instability occur at all, most of the hydrogen envelope must already have been stripped away, regardless of the details of how the star actually got into this state. The basic properties of our models at this stage of evolution are listed in Table 1, which contains somewhat improved values over those we calculated previously (SC94).

For our chosen initial stellar masses, the total lifetime of core helium burning is $(3-5) \times 10^5$ yr. The fraction of the post-main-sequence lifetime that is spent on the blue side of the H-R diagram is, for the adopted stellar wind mass-loss rates, equal to 0.6, 0.8, and ~ 1 in the cases of 30, 45, and 90 M_{\odot} , respectively. When a yellow or red phase of dynamical

instability occurs, its duration is at most $\sim 10^3$ yr and could be much shorter. The blue phase of dynamical instability lasts $\sim 10^4$ yr for initial masses of 45 M_{\odot} and 90 M_{\odot} , but is only $\sim 10^3$ yr for 30 M_{\odot} . These estimates were made by dividing the time-averaged rate of mass loss observed for LBVs (Lamers 1989) into the total amount of mass that must be removed from the models in order to permanently reestablish dynamical stability (§ 6). During the unstable period the star evolves on the H-R diagram as indicated by dashed lines in Figure 1. The numerous individual cycles of mass loss are not plotted, because during most of them the star remains a nearly stationary point on this diagram (SC95).

4. EVOLUTION OF MASSIVE METAL-POOR STARS

Dynamical instability does not develop before the red supergiant phase in our models of metal-poor stars with

TABLE 1
STELLAR MODELS AT THE START OF THE BLUE PHASE
OF DYNAMICAL INSTABILITY

| Initial M/M_{\odot} | Z | Remnant M/M_{\odot} | $\log(L/L_{\odot})$ | $\log T_e$ | Y_c |
|--------------------------|-------|--------------------------|---------------------|------------|-------|
| 30..... | 0.002 | 11 | a | a | a |
| | 0.004 | 11 | 5.54 | 3.84 | 0.002 |
| | 0.030 | 10 | 5.47 | 4.06 | 0.003 |
| 45..... | 0.002 | 20 | 5.85 | 3.86 | 0.01 |
| | 0.004 | 19 | 5.82 | 3.93 | 0.01 |
| | 0.030 | 18 | 5.75 | 4.12 | 0.03 |
| 90..... | 0.002 | 48 | 6.27 | 3.92 | 0.18 |
| | 0.004 | 46 | 6.26 | 4.01 | 0.26 |
| | 0.030 | 34 | 6.11 | 4.19 | 0.22 |

^a Star remains very blue and hence dynamically stable.

initial masses up to at least $120 M_{\odot}$, regardless of whether the modified or unmodified Nieuwenhuijzen & de Jager (1990) rates of stellar wind mass loss for hot stars are adopted. This result, while expected, is in sharp contrast to the case for massive stars with normal metallicities.

Once in the red region, however, the evolutionary patterns are similar. Stars lose mass rapidly, emerge as hydrogen-poor blue supergiants, and subsequently encounter dynamical instability when they are trying to reexpand. As Table 1 shows, the critical effective temperature is substantially lower for these metal poor stars than for stars with normal metallicities. Metal deficiency leads to reduced radiation pressure, and compensation for this stabilizing effect requires thicker ionization zones of hydrogen and helium in order to trigger the dynamical instability; the ionization zones become thicker only as the effective temperature decreases. In the extreme case of $Z = 0.002$ for $30 M_{\odot}$, the instability either never appears or else barely appears, depending sensitively on the amount of hydrogen remaining in the envelope.

Locations of our metal-poor models on the H-R diagram during the slow blue phase of dynamical instability are shown in Figure 2. Also plotted are our analogous models for $Z = 0.03$. The vertical line indicates the calculated threshold for dynamical instability that is imposed by the complete lack of *partially ionized* states of hydrogen and helium in a low-density envelope at effective temperatures higher than 30,000 K. Hotter stars are thus necessarily dynamically stable.

All models displayed are found to be relatively insensitive to the details of the prior evolution, except for two factors related to mass loss that still remain uncertain. One factor is the magnitude of the stellar wind mass-loss rate on the main sequence, which establishes the final mass of the helium core. However, for a fixed metallicity, the uncertainty in this

factor will primarily shift the models up and down the region of exhibited models on the H-R diagram, and will not much displace this region laterally. This important point has already been demonstrated for an initial mass of $90 M_{\odot}$ (SC95). In the case of initial masses below $\sim 60 M_{\odot}$, the final helium core mass is practically independent of the relatively inconsequential main-sequence stellar wind that prevails at lower luminosities.

A second uncertainty is the exact amount of hydrogen envelope remaining on the star. This uncertainty has only minor importance for estimating the star's total mass, since the mass fraction contained in the hydrogen envelope is small in any case. But the surface hydrogen abundance affects the stability of the outer envelope through the electron-scattering opacity (and, to a lesser extent, through the ionization thermodynamics). A smaller surface hydrogen abundance always increases the stability by lowering the opacity and hence by reducing the radiation pressure. Unless, however, the surface hydrogen abundance at the start of the blue phase of dynamical instability has been seriously overestimated in our calculations, all of the models shown in Figure 2 should be fairly accurately placed on the H-R diagram; their locations are otherwise not very sensitive to mild variations of the surface hydrogen abundance. The paradoxical decrease of stability with progressing evolution is due primarily to the rising luminosity of the star, whose plotted evolutionary track follows the theoretical line of marginal instability until nearly all the hydrogen is gone.

5. COMPARISON WITH OBSERVATIONS OF LBVS AT QUIESCENCE

Luminosities and effective temperatures of 14 well-observed LBVs at quiescence have been compiled by Humphreys & Davidson (1994, Table 4). Revised values for R71, due to Lennon et al. (1994), and for HR Car, due to Hutsemékers (1994), are adopted here. We also have added WRA 751 (Hu et al. 1990; Hutsemékers & Van Drom 1991b; van Genderen et al. 1992a). These 15 variables belong to five galaxies—the Milky Way, M31, M33, the LMC, and the SMC.

If the SMC is ignored for the moment, the four other galaxies exhibit mean Population I metallicities that probably range from ~ 0.01 to ~ 0.03 . When the LBVs are divided by galaxy, however, there is no obvious separation of them on the H-R diagram, most likely because the effect of the metallicity variation is too small to be detected amid the modest possible errors of the measured luminosities and effective temperatures. Therefore, we have plotted all these variables together in Figure 2. For the most part, they agree very well with our models for $Z = 0.03$ which are evolving in the blue phase of dynamical instability. Although our brightest theoretical models may be somewhat too cool, we note that the brightest LBVs show the most uncertain effective temperatures (Humphreys & Davidson 1994). In any case, no LBV is known to be hotter than 30,000 K, the ionization limit that our theory predicts.

The SMC variable R40 (Szeifert et al. 1993) is shown as the large "star" in Figure 2. This very metal-poor LBV is cooler than comparably bright LBVs containing a normal metals abundance, and falls close to the region occupied by our unstable models for $Z = 0.004$. Spectroscopic analyses of main-sequence B-type stars and other young objects in the SMC confirm that the average Population I metallicity

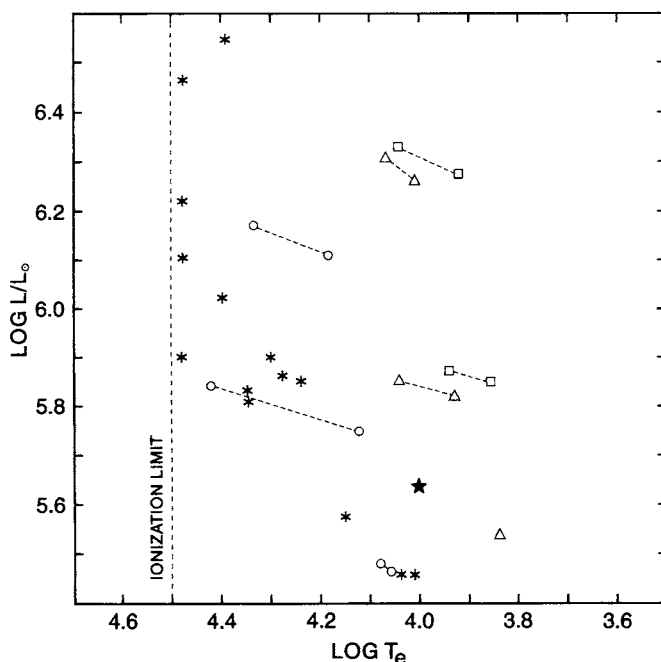


FIG. 2.—H-R diagram showing the location of stellar models during the second (blue) phase of dynamical instability for three metallicities: $Z = 0.03$, circles; $Z = 0.004$, triangles; and $Z = 0.002$, squares. Locations of observed LBVs at quiescence are also shown: normal metallicities, asterisks; low metallicities, large star.

TABLE 2
OBSERVED AND PREDICTED LUMINOSITY FUNCTIONS OF LUMINOUS BLUE VARIABLES

| INITIAL M/M_{\odot} | $\log(L/L_{\odot})$ | OBSERVED NUMBER BY GALAXY | | | | PREDICTED NUMBER |
|--------------------------|---------------------|---------------------------|-----|-------|-----|---------------------|
| | | MW | LMC | Other | All | |
| 60–100..... | 6.0–6.3 | 1 | 1 | 0 | 2 | 2 |
| 40–60..... | 5.7–6.0 | 2 | 3 | 2 | 7 | 8 |
| 30–40..... | 5.4–5.7 | 2 | 1 | 1 | 4 | 3 |
| 45–100..... | 5.8–6.2 | 3 | 4 | 2 | 9 | 9 |
| 30–45..... | 5.4–5.8 | 2 | 1 | 1 | 4 | 4 |

in this galaxy is lower than solar by 0.6 dex, or $Z \approx 0.004$ (Russell & Bessell 1989; Russell & Dopita 1990; Spite & Spite 1990; Luck & Lambert 1992; Thévenin & Jasiewicz 1992; Rolleston et al. 1993).

The luminosity function of the confirmed LBVs can be derived from Figure 2 and is listed in Table 2. We have truncated the distribution at $\log(L/L_{\odot}) = 6.3$, because the evolutionary status of the two brightest objects (η Car and AF And) is unclear. Since the relative luminosity function in the case of the best-studied galaxy, the LMC, is close to that for all the galaxies combined, selection effects can be regarded as being unimportant. We may therefore attempt to predict the luminosity function from the observed birthrate function of massive stars, combined with our theoretical lifetimes for the blue phase of dynamical instability. Since stellar associations probably form in sudden starbursts, the birthrate function should be approximately proportional to the initial mass function, which is observed to vary as M^{-2} in the stellar associations of the LMC and Milky Way (Blaha & Humphreys 1989; Parker & Garmany 1993). The resulting relative theoretical LBV luminosity function has been converted to an absolute luminosity function by assigning the same total number of stars as in the observed sample, and the results are entered in the last column of Table 2. Agreement with the observed function is very good, suggesting that the striking deficiency of fainter LBVs is not an observational selection effect but is rather the natural consequence of their shorter lifetime in this phase. The smallest luminosity observed for any LBV, including all of the still unconfirmed candidates (van Genderen et al. 1992b), is $\log(L/L_{\odot}) \approx 5.4$, which also agrees with the model predictions.

Masses of six confirmed LBVs have been derived spectroscopically from the stars' measured surface gravities, effective temperatures, and luminosities, viz., $M = gL/(4\pi G\sigma T_e^4)$. These published masses are listed in Table 3 and are displayed as a function of luminosity in Figure 3. In all cases, they lie well below the values expected for main-sequence

TABLE 3

SPECTROSCOPICALLY DERIVED MASSES OF LUMINOUS BLUE VARIABLES

| Variable | Galaxy | M/M_{\odot} | $\log(L/L_{\odot})$ | Reference |
|---------------|--------|---------------|---------------------|-----------|
| P Cyg..... | MW | 23 | 5.86 | 1, 2 |
| S Dor..... | LMC | 23 | 5.82 | 1, 3 |
| R71..... | LMC | 20 | 5.85 | 4 |
| R40..... | SMC | 16 | 5.64 | 5 |
| HD160529..... | MW | 13 | 5.46 | 1, 6 |
| R110..... | LMC | 10 | 5.46 | 1, 7 |

REFERENCES.—(1) Humphreys & Davidson 1994; (2) Pauldrach & Puls 1990; (3) Wolf & Stahl 1990; (4) Lennon et al. 1994; (5) Szeifert et al. 1993; (6) Sterken et al. 1991; (7) Stahl et al. 1990.

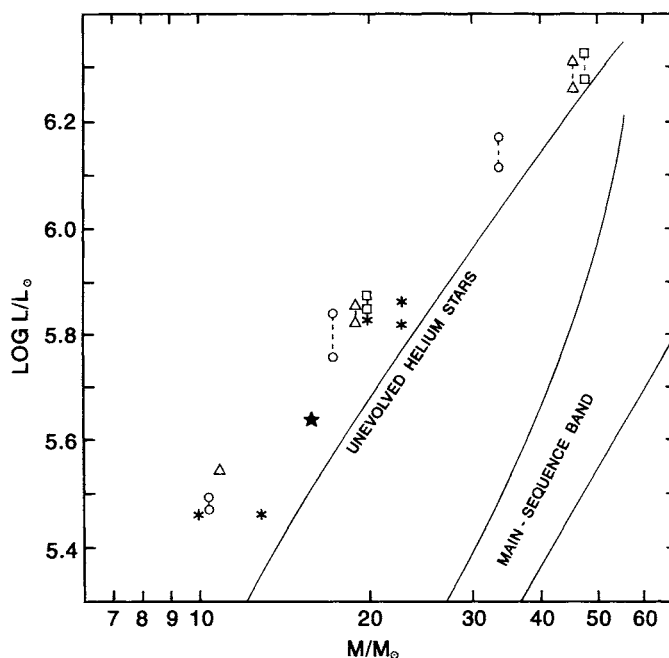


FIG. 3.—Mass vs. luminosity for observed LBVs and for theoretical LBV models evolving during the second (blue) phase of dynamical instability. Same notation as for Fig. 2.

stars, and imply the existence of substantial post-main-sequence mass loss. Our stellar models in the blue phase of dynamical instability define a thin band that virtually overlaps the band of observed stars. The theoretical (mass, luminosity) relation at the start of the blue phase can be represented by

$$\log(L/L_{\odot}) = 5.67 + 1.20 \log(M/15 M_{\odot}) \quad (1)$$

for $Z = 0.03$. For comparison, the observational relation is

$$\log(L/L_{\odot}) = (5.63 \pm 0.24) + (1.24 \pm 0.19) \log(M/15 M_{\odot}) \quad (2)$$

Uncertainty about the exact stage of interior evolution reached by each star affects our luminosity predictions, which could be slightly brighter than in equation (1). However, no significant metallicity dependence is either predicted or observed. The initial masses of the six plotted LBVs probably once spanned the range 30–60 M_{\odot} . Notice that the luminosities of the observed LBVs lie distinctly above the luminosities expected for unevolved helium stars,

a fact that points to an advanced stage of central helium depletion in these stars.

As noted in § 3, our prediction for the surface hydrogen abundance at the start of the blue phase of dynamical instability is fairly tightly constrained to a value that is significantly less than the zero-age main-sequence value. Our models formally show $X_{\text{surf}} = 0.22, 0.20,$ and 0.12 ± 0.04 for initial stellar masses of 30, 45, and $90 M_{\odot}$ with normal metallicities. Since X_{surf} must depend somewhat on the details of the uncertain prior history of mass loss, our derived values are probably compatible with the slightly higher hydrogen abundances measured for three LBVs: $X_{\text{surf}} = 0.36$ (Lennon et al. 1994) for R71; $X_{\text{surf}} = 0.33$ (Barlow 1991) or 0.38 (Langer et al. 1994) for P Cyg; and $X_{\text{surf}} = 0.49$ (Barlow 1991), 0.37 (Smith, Crowther, & Prinja 1994), or 0.18 (Leitherer et al. 1994) for AG Car. If the wide scatter of the published measurements for AG Car is representative of the total uncertainty for all three stars, our model predictions are in fact seen to be reasonably good.

6. NEBULAE SURROUNDING LBVS

During the yellow or red phase of dynamical instability, a very luminous star is expected to lose a large fraction of its mass in a single large ejection episode consisting of a series of closely spaced multiple outbursts. The estimated loss, ΔM , amounts to $4 \pm 1 M_{\odot}$ and $20 \pm 5 M_{\odot}$ for initial stellar masses of $45 M_{\odot}$ and $90 M_{\odot}$, respectively. If the mass lost is later detected as a nebula around the star during its blue phase of dynamical instability, the nebular mass should be related to the star's luminosity at that time in the following way: $\Delta M \propto L^{1.7 \pm 0.5}$. This prediction, which we have made previously (SC95), formally agrees in slope with Hutsemékers's (1994) observational relation for old nebulae surrounding LBVs, $\Delta M \propto L^{1.55 \pm 0.10}$.

Three difficulties, however, may scuttle this interpretation. First, old nebulae have been detected around some LBVs whose initial masses must have been as low as $30 M_{\odot}$. At least with the stellar wind mass-loss rates used here, our models do not go through a yellow or red phase of dynamical instability for stars with initial masses this low. Second, the observed nebular masses have been calibrated by using one absolutely measured value, $\sim 1\text{--}4 M_{\odot}$ for the AG Car nebula (Robberto et al. 1993). Our predicted value, corresponding to the observed luminosity of AG Car, is $\sim 20 M_{\odot}$, which is much too large if the empirical mass is roughly correct. Third, the expansion ages of the nebulae around five LBVs have been measured, and are 8×10^3 yr for AG Car (Robberto et al. 1993; Smith et al. 1994), $\sim 10^4$ yr for R71 (Roche, Aitken, & Smith 1993), $\sim 10^4$ yr for HR Car (Hutsemékers & Van Drom 1991a), 1.5×10^4 yr for WRA 751 (Hutsemékers & Van Drom 1991b), and 4×10^4 yr for R127 (Clampin et al. 1993). Ages this small are difficult to explain if the stars had been cool supergiants at the time they ejected the nebular material, because the intervening stages probably lasted $\sim 6 \times 10^4$ yr (§ 7).

A more realistic interpretation is that these nebulae constitute material ejected more or less continuously during the blue LBV phase itself. Indeed, the observed mean expansion age for these nebulae, $\sim 2 \times 10^4$ yr, is comparable to our theoretical estimate of the whole blue LBV lifetime.

It is not possible for us at the present time to predict the masses of the nebulae, except as to their general order. The remnant hydrogen envelopes in our models at the start of the blue phase of dynamical instability contain masses of

0.4, 0.6, and $1.2 M_{\odot}$ if the initial stellar mass was 30, 45, and $90 M_{\odot}$, respectively. On this basis, we might expect the nebula around AG Car to contain a mass of $1\text{--}2 M_{\odot}$, which is more or less the amount observed (Robberto et al. 1993). Nebular masses in general should increase with stellar mass and hence with stellar luminosity, but the theoretically predicted amount of matter actually removed from the star before the blue phase of dynamical instability ends is found to be proportionately less for a smaller initial stellar mass. Therefore, ΔM should increase somewhat more steeply than L , but we cannot make a more precise estimate at present.

An obvious prediction of our theory is that LBVs should also show older, more distant nebulae, which were produced during the earlier evolutionary phases when mass loss was also important. This point is discussed in the next section.

7. PRE-LBV AND POST-LBV STARS

The critical question of the magnitude of the stellar wind mass-loss rates for luminous red supergiants might be answered indirectly by using star count estimates of the ratio of times spent by post-main-sequence stars on the blue and red sides of the H-R diagram. The main difficulty lies in disentangling post-red-supergiant blue stars from main-sequence blue stars. Candidates for an evolved status have included Wolf-Rayet stars, LBVs, and B[e] supergiants. The simplest identification characteristic would be a very low surface hydrogen abundance.

Wolf-Rayet stars that display *mild* hydrogen deficiencies (the hydrogen-rich WN stars) are observed only at the highest luminosities, $\log(L/L_{\odot}) \geq 5.7$ (Hamann, Koesterke, & Wessolowski 1995; Crowther et al. 1995), and almost surely represent very massive main-sequence stars whose original outer envelopes have been stripped off by the powerful stellar wind before the end of central hydrogen burning (e.g., Tanaka 1966; Bressan et al. 1993; Meynet et al. 1994; Langer et al. 1994). Two other categories of Wolf-Rayet stars exist with luminosities in the LBV range: WN stars showing $X_{\text{surf}} = 0.1\text{--}0.3$ and WN/WC stars without detectable hydrogen. These objects are well matched by our models of pre-LBV and post-LBV stars, not only because the hydrogen abundances agree but also because our post-red-supergiant models spent most of their time at effective temperatures hotter than 25,000 K, i.e., in the Wolf-Rayet region. In fact, the hottest LBVs observed during their quiescent states look spectroscopically like hydrogen-poor WN stars (Smith et al. 1994).

If this line of reasoning is correct, the average expansion age of the small nebulae seen around some (presumed single) luminous hydrogen-poor WN stars, $\sim 6 \times 10^4$ yr (Marston 1995; Esteban & Rosado 1995), indicates that the post-red-supergiant phase must be rather brief and, therefore, that core helium burning must occur principally in the red supergiant region. Larger nebulae detected around some WN stars show a mean expansion age of $\sim 5 \times 10^5$ yr, which Marston (1995) has identified with the total duration of the red supergiant phase itself. This inferred age is certainly consistent with the total lifetime of core helium burning, which is $(3\text{--}5) \times 10^5$ yr according to our models. These larger nebulae are expected to contain the considerable mass that is lost in the red supergiant phase due to all causes, including a potential OH/IR phase of dynamical instability. A few massive yellow stars in transition out of the red supergiant region have also been identified by such

“fossil” dust shells (Roche et al. 1993; Jones et al. 1993; Kastner & Weintraub 1995).

It follows that the rates of stellar wind mass loss in the red region must be such that stars leave this region only toward the end of core helium burning. Rates of ~ 2 times the Nieuwenhuijzen & de Jager (1990) observational rates, rather than the larger factor of 5 that we assumed for our present evolutionary sequences, would be more appropriate. When the star has emerged from the red region and enters the WN domain, the rate of stellar wind mass loss becomes $\sim 4 \times 10^{-5} M_{\odot} \text{ yr}^{-1}$ (Hamann et al. 1995; Crowther et al. 1995; Nugis & Niedzielski 1995). Therefore in $\sim 6 \times 10^4$ yr, a WN star loses $\sim 2 M_{\odot}$. The hydrogen envelope in our $45 M_{\odot}$ sequence at the end of the red supergiant phase contains $3 M_{\odot}$, and this mass is probably fairly insensitive to the specific stage when the star exits the red region. Roughly $2 M_{\odot}$ are therefore available to lose before the star becomes a LBV. Theory and observation are accordingly consistent.

Among the less-luminous WN stars, only one hydrogen-poor member is known to occur in the luminosity range $\log(L/L_{\odot}) = 5.4\text{--}5.6$, even though numerous hydrogen-free objects exist there (Hamann et al. 1995; Crowther et al. 1995). The lifetime of the pre-LBV blue phase for stars belonging to the corresponding initial mass range, $30\text{--}40 M_{\odot}$, must therefore be much shorter than for the more massive objects. This is consistent with the fact that our $30 M_{\odot}$ sequence has only $\sim 0.7 M_{\odot}$ available to lose during the pre-LBV phase. Another important inference is that the red supergiant mass-loss rates would have to be ~ 2 times the Nieuwenhuijzen & de Jager (1990) observational rates. Vanbeveren (1995) has recently inferred a larger factor of ~ 10 from considerations of the observed numbers of O stars and Wolf-Rayet stars, both single and binary, in the Galaxy and Magellanic Clouds, but partly interpreted with the help of evolutionary tracks. Because our factor of ~ 2 is based on simpler and more direct observational considerations, without the need for theoretical stellar models, we regard it as more likely to be correct.

Since no single WN star is known to be brighter than $\log(L/L_{\odot}) = 6.0$, the post-main-sequence fate of stars initially more massive than $\sim 60 M_{\odot}$ cannot yet be determined empirically. Our $90 M_{\odot}$ sequence predicts that the whole of core helium burning occurs on the blue side of the H-R diagram after the rapid yellow (or red) phase of dynamical instability ends. Whether or not the object becomes a hydrogen-poor WN star depends critically on the rate of mass loss assumed for the *main-sequence* phase. Using the Nieuwenhuijzen & de Jager (1990) main-sequence rates, we find that the star does finally enter the hydrogen-poor WN domain (Fig. 1). However, with a main-sequence mass loss rate smaller by a factor of 3, which is not impossible (Lamers & Leitherer 1993), the hydrogen-poor descendant always remains cooler than 25,000 K. Nevertheless, in both cases, calculations show that the star eventually evolves into a LBV with a remnant hydrogen envelope of $\sim 1 M_{\odot}$.

It is by now obvious that no room is left to place the numerous B[e] supergiants of high luminosity among the post-red-supergiant stars. The only alternative is that most, if not all, of these B[e] supergiants are located in, but close to the end of, the main-sequence phase, because their relatively large numbers imply lifetimes of at least $(1\text{--}2) \times 10^5$ yr, while their effective temperatures are only as high as 25,000 K or lower (Zickgraf 1989; Zickgraf, Stahl, & Wolf

1992). These objects may well be the cool counterparts of the hydrogen-rich WN stars. A critical test of our theory, at least in its present form, would be an accurate determination of the surface hydrogen abundance for a few luminous B[e] supergiants. If these stars indeed lie on the greatly widened main sequence that exists at high luminosities, their hydrogen abundances ought to be more or less normal.

8. CONCLUSION

In the conventional scheme of stellar evolution, the LBVs have found a place as follows:

O \rightarrow Of \rightarrow BSG (or H-rich WN) \rightarrow

LBV \rightarrow WN \rightarrow WC \rightarrow SN ,

where the abbreviations are O for O-type star, Of for Of star, BSG for blue supergiant, and SN for supernova (e.g., Sterken & Wolf 1978; Humphreys & Davidson 1979; Schaller et al. 1992; Bressan et al. 1993; Meynet et al. 1994). In all versions of this scheme, the LBV phase occurs during (or shortly after) the main-sequence phase, produces an enormous loss of mass, and prevents evolution to the red. No explicitly demonstrated mechanism of mass loss, however, has been discovered that actually supports this scheme. The time-averaged empirical rates of mass loss from LBVs, in fact, are nowhere near high enough to be relevant (Lamers 1989; Humphreys & Davidson 1994).

Several modifications of the traditional scheme have, nevertheless, recently come from Langer et al. (1994). These authors have noted that modern models of massive stars contain a large number of excited radial dynamical strange modes (Kiriakidis, Fricke, & Glatzel 1993). Although these modes are not the same phenomenon as our classical dynamical instability and actually have still unknown astrophysical consequences, Langer et al. assumed that they can pulsationally induce mass loss at a fast rate. An initial stellar mass of $60 M_{\odot}$ was adopted in their work. Since the strange modes are most unstable in the effective temperature range 22,000–42,000 K at $60 M_{\odot}$, enhanced mass loss was assumed to take place at these temperatures; the corresponding stellar luminosities were $\log(L/L_{\odot}) = 5.7\text{--}5.9$. The following sequence of stellar types emerged from their calculations:

O \rightarrow Of \rightarrow H-rich WN \rightarrow LBV \rightarrow H-poor WN \rightarrow

H-free WN \rightarrow WC \rightarrow SN .

Although their estimates of the surface hydrogen abundances for LBVs lie in the acceptable range, the predicted effective temperatures ($\log T_e = 3.6\text{--}4.6$) and masses ($M/M_{\odot} = 20\text{--}28$) cover much wider ranges than those observed (cf. Figs. 2 and 3). Moreover, the models do not yield anything like the observed cycles of mass loss. Specific predictions have not yet been made for other initial stellar masses or for nonsolar initial metallicities.

The fainter LBVs have long posed a theoretical problem, because at their luminosities red supergiants do exist. Lamers, de Groot, & Cassatella (1983) were the first to suggest that these LBVs arose from red supergiants by mass loss during the early stages of core helium burning. They proposed:

O \rightarrow Of \rightarrow RSG \rightarrow LBV \rightarrow WN \rightarrow WC? \rightarrow SN .

Their idea, as contrasted with the conventional scheme, implies the existence of a fundamental difference between brighter and fainter LBVs. Since observations have not yet supported such a difference, at least for $\log(L/L_{\odot}) < 6.3$, we suspect that the conventional scheme, in which the LBV phase itself is the site of major mass loss, is somehow wrong.

Our new work has led to a very different scheme of evolution. For initial masses of $\sim 60\text{--}90 M_{\odot}$, we predict

O \rightarrow Of \rightarrow H-rich WN \rightarrow H-rich B[e] \rightarrow YSG
 \rightarrow Yellow LBV \rightarrow H-poor WN (or H-poor B[e])
 \rightarrow Blue LBV \rightarrow H-free WN \rightarrow WC \rightarrow SN .

For $\sim 30\text{--}60 M_{\odot}$, we propose

O \rightarrow Of \rightarrow H-rich B[e] \rightarrow RSG \rightarrow Red LBV \rightarrow H-poor WN
 \rightarrow H-poor B[e] \rightarrow Blue LBV \rightarrow H-free WN \rightarrow WC \rightarrow SN .

In the case of metal-poor stars of $\sim 30\text{--}90 M_{\odot}$, only the second scheme applies. For the moment, the WC link is still conjectural, because our models have not yet been carried further than the second (blue) LBV phase. Observed luminosities of the WC stars (Koesterke & Hamann 1995), however, support such a conjecture, as also do the applicable final segments of the evolutionary tracks computed by other authors (Schaller et al. 1992; Bressan et al. 1993; Meynet et al. 1994; Langer et al. 1994).

The following points of detailed agreement with observations have been achieved by our models, up to luminosities of roughly $\log(L/L_{\odot}) = 6.3$:

1. A demonstrable mechanism (ionization-induced dynamical instability) exists in the stellar models. It triggers rapidly growing relaxation oscillations with periods of a few months, which are expected to expel matter from the surface until dynamical stability is reestablished (SC93).

2. This dynamical instability can occur during two different evolutionary phases: once, briefly, either just before the start or during the main stages of central helium burning, when the star is a yellow or red supergiant; and later, for a much longer time, toward the end of central helium burning, when the star is again a blue supergiant. Nearly all LBVs are predicted to be in the blue supergiant phase (SC94).

3. The LBV phase does not occur before, or even at, the terminus of the main sequence. The main-sequence terminus is probably to be identified with the empirical Humphreys & Davidson (1979) line on the H-R diagram (SC93; SC94).

4. Slow cycles of alternating eruption and quiescence occur quasi-regularly on an annual-to-decadal (rarely centuries) timescale. During the course of most of these cycles, the star moves hardly at all on the H-R diagram, the observable changes being produced primarily by the optically thick ejected cloud. For P Cyg, however, the rate of decrease of effective temperature following the star's unusually high seventeenth-century activity has been measured (Lamers & de Groot 1992) and is reproduced well by our models. Eruptive mass loss rates (for all but the very brightest LBVs) are nearly independent of stellar luminosity, and may be not much greater than the quiescent rates. The lengths of the observed and predicted cycles for each star, though occasionally as great as centuries, have a

small enough variance that a meaningful "period" can be assigned. This period is inversely proportional to the star's luminosity (SC95).

5. A narrow band on the H-R diagram contains the dynamically unstable blue supergiant models; it runs diagonally toward hotter effective temperatures and higher luminosities. A theoretical upper limit to the effective temperature of these models is 30,000 K. A lower limit to the luminosities occurs at $\log(L/L_{\odot}) \approx 5.4$, corresponding to an initial stellar mass of $\sim 30 M_{\odot}$.

6. Metal-poor LBVs are significantly cooler, at a given luminosity, than LBVs with normal metallicities.

7. On the (mass, luminosity) plane, LBVs occupy a thin strip that represents very nearly the locus of massive, hydrogen-free helium stars in an advanced stage of central helium depletion.

8. Surface hydrogen abundances in most LBVs are predicted to be $X_{\text{surf}} = 0.2 \pm 0.1$.

9. Pre-LBV and post-LBV stars should appear as hydrogen-poor WN and hydrogen-free WN stars, respectively.

10. Lifetimes of the LBV and associated WN phases have been derived from the observed numbers of these stars and from the kinematical ages of their surrounding nebulae. For initial stellar masses less than $\sim 60 M_{\odot}$, the short LBV/WN lifetimes imply a long stay on the red supergiant branch. We infer average rates of stellar wind mass loss from red supergiants of ~ 2 times the Nieuwenhuijzen & de Jager (1990) observational rates. For initial stellar masses greater than $\sim 60 M_{\odot}$, virtually all of the post-main-sequence lifetime is spent on the blue side of the H-R diagram.

11. The LBV phase is not the place where the major mass loss from massive stars occurs. (It occurs during the preceding yellow or red supergiant phase.) In their lifetimes of $10^3\text{--}10^4$ yr, however, LBVs do build up surrounding nebulae with masses of $\sim 0.4\text{--}1.2 M_{\odot}$, the larger masses being associated with the more luminous stars.

12. The lifetime of the LBV phase increases with initial stellar mass, leading to an "inverted" luminosity function in which fainter LBVs are less frequent.

Among the successes of the present theory, there are inevitably a few discrepancies with observations. These may perhaps be treated as new predictions and are enumerated here. No known stars brighter than $\log(L/L_{\odot}) = 5.8$ lie to the right of the Humphreys-Davidson line on the H-R diagram, although a very small percentage of stars should exist there with spectral types later than middle B. Observed effective temperatures of quiescent-state LBVs brighter than $\log(L/L_{\odot}) = 6.0$, although rather uncertain (Humphreys & Davidson 1994), lie somewhat above our predicted values. Measured surface hydrogen abundances in LBVs likewise exceed by a modest amount our model values, but possess potentially large errors. Distant nebulae ought to be detectable around LBVs; our theory predicts three additional phases of heavy mass loss, when the precursor to the LBV was a hydrogen-poor WN star, a yellow or red supergiant, and a main-sequence star. Luminous B[e] supergiants are interpreted as being, for the most part, main-sequence stars with essentially normal surface hydrogen abundances; the observational evidence concerning their evolutionary status is still ambiguous. Finally, our theoretical models, like other authors' models, still provide no clue to the source of the exceptionally high mass-loss rates in Wolf-Rayet stars or to

the evolutionary origin of the many Wolf-Rayet stars with luminosities fainter than $\log(L/L_{\odot}) = 5.4$.

The evolution of extremely massive stars with $\log(L/L_{\odot}) > 6.3$ has not yet been studied in the framework of our theory. At such high luminosities, the enormous quantity of main-sequence mass loss must dominate the star's

evolution, and so is expected to control the development of the LBV phase.

The OPAL opacity tables were kindly supplied to us by Forrest J. Rogers. Our work has been supported by the NASA Astrophysics Research Program.

REFERENCES

- Barlow, M. J. 1991, in IAU Symp. 143, Wolf-Rayet Stars and Interrelations with Other Massive Stars in Galaxies, ed. K. A. Van der Hucht & B. Hidayat (Dordrecht: Kluwer), 281
- Blaha, C., & Humphreys, R. M. 1989, *AJ*, 98, 1598
- Bressan, A., Fagotto, F., Bertelli, G., & Chiosi, C. 1993, *A&AS*, 100, 647
- Clampin, M., Nota, A., Golimowski, D. A., Leitherer, C., & Durrance, S. T. 1993, *ApJ*, 410, L35
- Conti, P. S. 1984, in IAU Symp. 105, Observational Tests of Stellar Evolution Theory, ed. A. Maeder & A. Renzini (Dordrecht: Reidel), 233
- Crowther, P. A., Smith, L. J., Hillier, D. J., & Schmutz, W. 1995, *A&A*, 293, 427
- Dupree, A. K. 1986, *ARA&A*, 24, 377
- Esteban, C., & Rosado, M. 1995, *A&A*, 304, 491
- Hamann, W.-R., Koesterke, L., & Wessolowski, U. 1995, *A&A*, 299, 151
- Hu, J. Y., de Winter, D., Thé, P. S., & Pérez, M. R. 1990, *A&A*, 227, L17
- Humphreys, R. M. 1989, in *Physics of Luminous Blue Variables*, ed. K. Davidson, A. F. J. Moffat, & H. J. G. L. M. Lamers (Dordrecht: Kluwer), 3
- Humphreys, R. M., & Davidson, K. 1979, *ApJ*, 232, 409
- . 1994, *PASP*, 106, 1025
- Hutsemékers, D. 1994, *A&A*, 281, L81
- Hutsemékers, D., & Van Drom, E. 1991a, *A&A*, 248, 141
- . 1991b, *A&A*, 251, 620
- Iglesias, C. A., Rogers, F. J., & Wilson, B. G. 1992, *ApJ*, 397, 717
- Jones, T. J., et al. 1993, *ApJ*, 411, 323
- Jura, M., & Kleinmann, S. G. 1990, *ApJS*, 73, 769
- Kastner, J. H., & Weintraub, D. A. 1995, *ApJ*, 452, 833
- Kiriakidis, M., Fricke, K. J., & Glatzel, W. 1993, *MNRAS*, 264, 50
- Koesterke, L., & Hamann, W.-R. 1995, *A&A*, 299, 503
- Lamers, H. J. G. L. M. 1989, in *Physics of Luminous Blue Variables*, ed. K. Davidson, A. F. J. Moffat, & H. J. G. L. M. Lamers (Dordrecht: Kluwer), 135
- Lamers, H. J. G. L. M., & de Groot, M. J. H. 1992, *A&A*, 257, 153
- Lamers, H. J. G. L. M., de Groot, M., & Cassatella, A. 1983, *A&A*, 123, L8
- Lamers, H. J. G. L. M., & Leitherer, C. 1993, *ApJ*, 412, 771
- Langer, N., Hamann, W.-R., Lennon, M., Najarro, F., Pauldrach, A. W. A., & Puls, J. 1994, *A&A*, 290, 819
- Ledoux, P. 1958, in *Handbuch der Physik*, Vol. 51, ed. S. Flügge (Berlin: Springer), 605
- Leitherer, C., Robert, C., & Drissen, L. 1992, *ApJ*, 401, 596
- Leitherer, C., et al. 1994, *ApJ*, 428, 292
- Lennon, D. J., Wobig, D., Kudritzki, R.-P., & Stahl, O. 1994, *Space Sci. Rev.*, 66, 207
- Luck, R. E., & Lambert, D. L. 1992, *ApJS*, 79, 303
- Marston, A. P. 1995, *AJ*, 109, 1839
- Meynet, G., Maeder, A., Schaller, G., Schaerer, D., & Charbonnel, C. 1994, *A&AS*, 103, 97
- Nieuwenhuijzen, H., & de Jager, C. 1990, *A&A*, 231, 134
- Nugis, T., & Niedzielski, A. 1995, *A&A*, 300, 237
- Parker, J. W., & Garmany, C. D. 1993, *AJ*, 106, 1471
- Pauldrach, A. W. A., & Puls, J. 1990, *A&A*, 237, 409
- Robberto, M., Ferrari, A., Nota, A., & Paresce, F. 1993, *A&A*, 269, 330
- Roche, P. F., Aitken, D. K., & Smith, C. H. 1993, *MNRAS*, 262, 301
- Rolleston, W. R. J., Dufton, P. L., Fitzsimmons, A., Howarth, I. D., & Irwin, M. J. 1993, *A&A*, 277, 10
- Russell, S. C., & Bessell, M. S. 1989, *ApJS*, 70, 865
- Russell, S. C., & Dopita, M. A. 1990, *ApJS*, 74, 93
- Schaller, G., Schaerer, D., Meynet, G., & Maeder, A. 1992, *A&AS*, 96, 269
- Smith, L. J., Crowther, P. A., & Prinja, R. K. 1994, *A&A*, 281, 833
- Spite, M., & Spite, F. 1990, *A&A*, 234, 67
- Stahl, O., Wolf, B., Klare, G., Jüttner, A., & Cassatella, A. 1990, *A&A*, 228, 379
- Sterken, C., Gosset, E., Jüttner, A., Stahl, O., Wolf, B., & Axer, M. 1991, *A&A*, 247, 383
- Sterken, C., & Wolf, B. 1978, *A&A*, 70, 641
- Stothers, R. B., & Chin, C.-w. 1993, *ApJ*, 408, L85 (SC93)
- . 1994, *ApJ*, 426, L43 (SC94)
- . 1995, *ApJ*, 451, L61 (SC95)
- Szeifert, T., Stahl, O., Wolf, B., Zickgraf, F.-J., Bouchet, P., & Klare, G. 1993, *A&A*, 280, 508
- Tanaka, Y. 1966, *Prog. Theor. Phys.*, 36, 844
- Thévenin, F., & Jasniewicz, G. 1992, *A&A*, 266, 85
- Vanbeveren, D. 1995, *A&A*, 294, 107
- van Genderen, A. M., Thé, P. S., de Winter, D., Hollander, A., de Jong, P. J., van den Bosch, F. C., Kolkman, O. M., & Verheijen, M. A. W. 1992a, *A&A*, 258, 316
- van Genderen, A. M., et al. 1992b, *A&A*, 264, 88
- Wolf, B. 1991, in IAU Symp. 148, The Magellanic Clouds, ed. R. Haynes & D. Milne (Dordrecht: Kluwer), 266
- Wolf, B., & Stahl, O. 1990, *A&A*, 235, 340
- Zickgraf, F.-J. 1989, in *Physics of Luminous Blue Variables*, ed. K. Davidson, A. F. J. Moffat, & H. J. G. L. M. Lamers (Dordrecht: Kluwer), 117
- Zickgraf, F.-J., Stahl, O., & Wolf, B. 1992, *A&A*, 260, 205